ANALYSIS OF DEMAGNETIZATION FAULT BACK-EMF OF PERMANENT MAGNET SYNCHRONOUS MOTOR USING MATHEMATICAL MODEL BASED ON MAGNETIC FIELD SUPERPOSITION PRINCIPLE

Zhiyan Zhang[1], Zehui Xie[1], Hongzhong Ma[2], Qin Zhong[3]
[1] – Zhengzhou University of Light Industry, College of Electrical and Information Engineering, Dongfeng Road No. 5 Zhengzhou City Henan Province China.
e-mail: 2004074@zzuli.edu.cn; 2000002@zzuli.edu.cn
[2] – College of Energy and Electrical Engineering, Hohai University, Fucheng West Road No. 8 Nanjing City Jiangsu Province, 210098, China. e-mail: Hongzhong Ma@163.com
[3] – Huzhou Power Company, Electric Power Company of Zhejiang Province, Fenghuang Road No.777 Huzhou City Zhejiang Province, 313000, China. e-mail: hhupszq@163.com

According to magnetic field superposition principle and characteristic of square wave series, back-EMF of permanent magnet synchronous motor (PMSM) under demagnetization fault condition is decomposed into health component and demagnetization fault component. A operation of mathematical model of single slot and single phase no-load back-EMF, when demagnetization fault of different degree occurred in any magnetic body, any single pole and any multiple pole, is presented. The back-EMF mathematical model and the finite element simulation model results for 42 kW - PMSM, which has 8 poles and V-shaped permanent magnet rotor structure are compared, that allowed to verify the mathematical model. The results show that the back-EMF waveform of the slot winding can reflect the specific position and the severity of the demagnetization poles. The single phase back-EMF waveform can reflect only demagnetization conditions of all poles, but can not identify the specific position of the demagnetization poles. References 9, figures 5.
Key words: PMSM; demagnetization fault; back-EMF; mathematical model; simulation model.

I. Introduction. PMSM has the characteristics of compact structure, small volume, light weight, high efficiency, high torque, high power density, high reliability, low noise and so on. It has the best comprehensive index of electric vehicle (EV) drive motor, which is very suitable for EV drive field [1, 3−5]. The drive motor is an important part of EV whose reliability can directly affect not only the vehicle performance, and even endanger the safety of human life. The electromagnetic, thermal and mechanical stress [2] under the harsh working environment or complication operating conditions induces demagnetization of the PMSM permanent magnet. Once the permanent magnet has irreversible demagnetization, the PMSM performance is deteriorated and evenly may be out of control and out of survives [6, 8−9]. Therefore, PMSM's application has been greatly limited in harsh environment and high reliability requirement.

At present, there are many researches that have studied the demagnetization fault influence of the PMSM performance and demagnetization fault diagnosis method, and most of which focus on permanent magnet demagnetization curve based on demagnetization fault model [7], but the research on the mathematical model of PMSM demagnetization fault is less. The mathematical model of the single slot back-EMF under no-load conditions of the surface PMSM is given in [3]. In this paper, a 42 kW PMSM is studied. The mathematical model of the no-load back-EMF is developed, and the finite element model (FEM) is built to simulate the demagnetization fault. At last, the validity of the model is verified by comparison the results of mathematical model and FEM model.

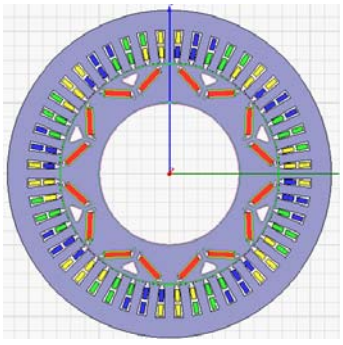

Fig. 1

PMSM partial demagnetization model. In order to analyze the mathematical model of PMSM, an EV drive motor is studied. The number of the PMSM poles is 8, the distribution of magnets is built-in V-shaped, the stator structure is double-layer with 48 slots, the number of parallel branches are 8, all which makes the winding electromotive force closer to sine wave; its main performance parameters are that the rated power is 42 kW, the rated speed of 3000r/min, the rated input voltage 375 V provided by the inverter and the control model is direct torque control. The complete finite element analysis model using Ansoft/Maxwell software is established as is shown in Fig. 1.

For convenience of analysis the PMSM poles are numbered. A-phase winding is numbered according to counterclockwise direction as shown in Fig. 2. Fig. 2 shows that the direction of the coil current is specified, the inflow is positive, and the outflow is negative. All the upper lines of the PMSM are connected together, all

the lower lines of the PMSM are also connected together, then A, B, C three-phase end are connected by the Y connection structure. The solid lines represent the upper coil side, the dotted lines represent the lower coil side, and the arrows represent flows.

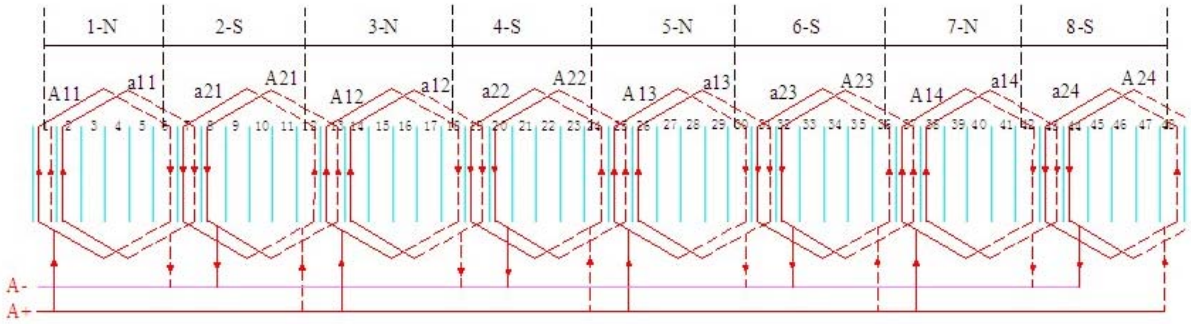

Fig. 2

Theoretical basis of PMSM partial demagnetization mathematic model. The PMSM simulation method is applied on pole 1 in three ways which are normal, 25% demagnetization and 50% demagnetization of the PMSM. The slot winding back-EMF under no-load operation is studied and it is shown in Fig. 3. Fig.3 shows that when the fault pole 1 moves over A1 slot, the amplitude of slot winding back-EMF is reduced, and the magnitude of the reduction is increased with the increase of the fault severity. When the healthy pole moves over A1 slot, the back-EMF waveform and amplitude are not changed.

In order to simplify analysis, no-load back-EMF harmonics are ignored, only single slot back-EMF fundamental component is considered. The no-load single slot back-EMF instantaneous value can be get at the rated speed marked with the symbol e_s. On the basis of the FEM simulation analysis, in Fig. 3 pole 1 occurs 25% demagnetization fault, when the pole 1 moves over A1 slot, the slot winding back-EMF amplitude decreases and waveform changes, and it can be regarded as normalized sine wave $e_s(t)/E_s$ minus $y(t)$ wave results (Fig. 4). The slot winding back-EMF fundamental amplitude under no-load operation is expressed as the symbol E_s, the demagnetization fault effect on slot winding back-EMF is expressed as the symbol $y(t)$. The demagnetization fault position is simulated by the square wave $x(t)$. Based on this, the A1 slot back-EMF fundamental waveform under the pole 1 demagnetization fault condition is shown in Fig. 4, in which the back-EMF waveform is normalized.

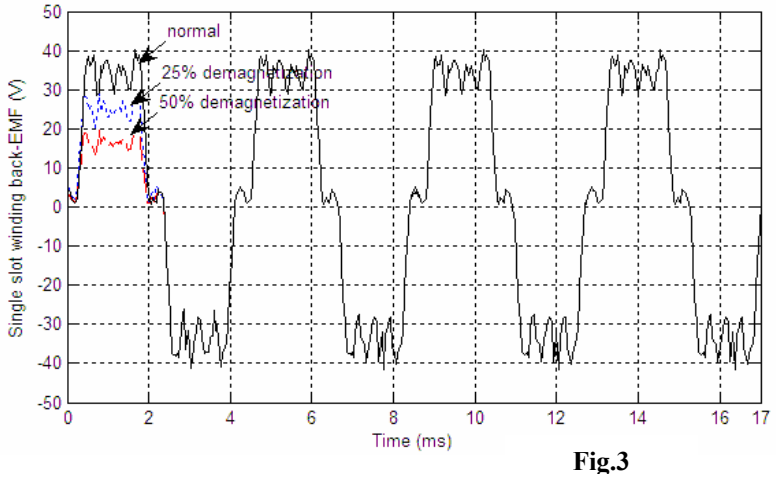

Fig.3

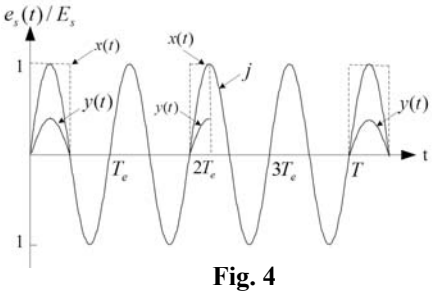

Fig. 4

In Fig 4, $x(t)$ is A1 slot corresponding square wave under pole 1 occurred demagnetization fault. The amplitude of the square wave is 1 when pole 1 moves over A1 slot, and the amplitude of the square wave is zero when the other poles move over it. Fourier series of square wave can be expressed as follows

$$x(t) = \frac{1}{2p} + \sum_{n=1}^{\infty} \frac{2}{n\pi} \sin\frac{n\pi}{2p} \cos\left(\frac{2n\pi fet}{p} - \frac{n\pi}{2p}\right), \quad (1)$$

where p is the pole numbers of PMSM; f_e is the rated frequency of PMSM; T is the mechanical period of the motor; T_e is the induction period of the motor. In Fig. 4, $y(t)$ is product of K_1, sine fundamental wave and square wave $x(t)$, when pole 1 moves over A1 slot, the no-load back-EMF fundamental waveform amplitude is reduced by K_1, so $y(t)$ can be expressed as follows.

$$y(t)=K_1\sin(2\pi fet)\left\{\frac{1}{2p}+\sum_{n=1}^{\infty}\frac{2}{n\pi}\sin\frac{n\pi}{2p}\cos[\frac{2n\pi fet}{p}-\frac{n\pi}{2p}]\right\}=$$
$$=-\frac{K_1}{2p}\sin(2\pi fet)+K_j\sum_{n=1}^{\infty}\frac{1}{n\pi}\sin\frac{n\pi}{2p}\cos[2\pi fet(1\pm\frac{n}{p})\mp\frac{n\pi}{2p}], \quad (2)$$

where K_1 is the percentage of the magnetic density's reduction of the original value after pole 1 temperature recovery, namely pole 1 demagnetization fault level, and $0\le K_1\le 1$.

The above mentioned analysis shows that slot winding fundamental back-EMF at normal steady-state no-load operation minus the demagnetization fault corresponds to wave $y(t)$, namely the slot winding no-load back-EMF under demagnetization fault state. Therefore, when the j pole demagnetization fault occurred, the A1 slot back-EMF mathematical model under no-load condition can be expressed as

$$e_{s,A1}(t)/E_S=\sin(2\pi f_e t)-y(t), \quad (3)$$

where E_S is the fundamental value of the slot winding back-EMF under no-load operation, written as $E_S=2\pi f_e N\phi_1$; N is the number of the slot windings; ϕ_1 is the main flux of the fundamental wave under no-load condition.

Slot winding back-EMF mathematical model under any single magnet demagnetization.

A. The j_1 magnetic body of the j pole demagnetization fault.

Where j_1 and j_2 respectively represent the first and the second magnetic body of the j pole, if the j_1 demagnetization, the waveforms is shown in Fig. 4. Fig. 4 shows that the j_1 magnetic body corresponding square-wave internal is $[\frac{j-1}{2f_e},\frac{2j-1}{4f_e}]$, and the Fourier series of the corresponding square wave signals can be represented as (4)

$$x1(t)=\frac{1}{4p}+\sum_{n=1}^{\infty}\frac{2}{n\pi}\sin\frac{n\pi}{4p}\cos[\frac{2n\pi fet}{p}-\frac{(4j-3)n\pi}{4p}]. \quad (4)$$

$y1(t)$ is product of K_{j1}, sine fundamental wave and square wave $x1(t)$. On the basis of previous theoretical analysis, the mathematical model of $y1(t)$ is established and can be expressed as follows

$$y1(t)=K_{j1}\sin(2\pi fet)\left\{\frac{1}{4p}+\sum_{n=1}^{\infty}\frac{2}{n\pi}\sin\frac{n\pi}{4p}\cos[\frac{2n\pi fet}{p}-\frac{(4j-3)n\pi}{4p}]\right\}=$$
$$=-\frac{K_{j1}}{4p}\sin(2\pi fet)+K_j\sum_{n=1}^{\infty}\frac{1}{n\pi}\sin\frac{n\pi}{4p}\cos[2\pi fet(1\pm\frac{n}{p})\mp\frac{(4j-3)n\pi}{4p}]. \quad (5)$$

In the same way, the mathematical model of no-load A1 slot winding back-EMF under the j_1 magnetic body demagnetization can be expressed as follows

$$e1_{s,A1}(t)=E_S(1-\frac{K_{j1}}{4p})\sin(2\pi f_e t)-E_S K_{j1}\sum_{n=1}^{\infty}\frac{1}{n\pi}\sin\frac{n\pi}{4p}[\sin 2\pi fet(1\pm\frac{n}{p})\mp\frac{(4j-3)n\pi}{4p}]. \quad (6)$$

The Fourier series of the a1 slot which is adjacent to the A1 slot corresponding square wave signals can be expressed as follows

$$x1(t)=\frac{1}{4p}+\sum_{n=1}^{\infty}\frac{2}{n\pi}\sin\frac{n\pi}{4p}\cos[\frac{2n\pi fet}{p}-\frac{(4j-3)n\pi+4n\alpha)}{4p}]. \quad (7)$$

The mathematical model of adjacent slot a1 back-EMF under the magnetic body j_1 demagnetization fault can be expressed as follows

$$e1_{s,a1}(t)=E_S(1-\frac{K_{j1}}{4p})\sin(2\pi f_e t)-E_S K_{j1}\sum_{n=1}^{\infty}\frac{1}{n\pi}\sin\frac{n\pi}{4p}\times[\sin 2\pi fet(1\pm\frac{n}{p})\mp\frac{(4j-3)n\pi+4n\alpha}{4p}]. \quad (8)$$

B. The j_2 magnetic body of the j pole demagnetization fault.

Fig. 4 shows that the j_2 magnetic body corresponding square-wave internal is $[\frac{2j-1}{4f_e},\frac{j}{2f_e}]$, and the Fourier series of the corresponding square wave signals can be expressed as follows

$$x2(t) = \frac{1}{4p} + \sum_{n=1}^{\infty} \frac{2}{n\pi} \sin\frac{n\pi}{4p} \cos[\frac{2n\pi f_e t}{p} - \frac{(4j-1)n\pi}{4p}]. \quad (9)$$

In the same way, the mathematical model of A1 slot and the adjacent a1 slot winding no-load back-EMF under the j_2 magnetic body demagnetization condition can be expressed as follows

$$e2_{s,A1}(t) = E_S(1 - \frac{K_{j2}}{4p})\sin(2\pi f_e t) - E_S K_{j2} \sum_{n=1}^{\infty} \frac{1}{n\pi} \sin\frac{n\pi}{4p} \sin[2\pi f_e t(1 \pm \frac{n}{p}) \mp \frac{(4j-1)n\pi}{4p}]; \quad (10)$$

$$e2_{s,a1}(t) = E_S(1 - \frac{K_{j2}}{4p})\sin(2\pi f_e t) - E_S K_{j2} \sum_{n=1}^{\infty} \frac{1}{n\pi} \sin\frac{n\pi}{4p} \sin[2\pi f_e t(1 \pm \frac{n}{p}) \mp \frac{(4j-1)n\pi + 4n\alpha)}{4p}]. \quad (11)$$

Slot winding back-EMF mathematical model under demagnetization of any single pole or multiple ones.

A. Slot winding back-EMF mathematical model under any single pole demagnetization.

Any single pole demagnetization, which is both j_1 and j_2 magnetic body of the j pole occurred demagnetization fault. According to (3), (6) and (10), the no-load back-EMF mathematical model of the A1 slot winding can be expressed as follows

$$e_{s,A1}(t) = el_{s,A1}(t) + e2_{s,A1}(t) - E_S \sin(2\pi f_e t). \quad (12)$$

After subotitution (6) and (11) into (12), and it can be simplified as follows

$$\begin{aligned} e_{s,A1}(t) = E_S(1 - \frac{K_{j1} + K_{j2}}{4p})\sin(2\pi f_e t) - E_S \sum_{n=1}^{\infty} \frac{1}{n\pi} \Big\{ K_{j1} \sin\frac{n\pi}{4p} \times \\ \times \sin[2\pi f_e t(1 \pm \frac{n}{p}) \mp \frac{(4j-3)n\pi}{4p}] + K_{j2} \sin\frac{n\pi}{4p} \sin[2\pi f_e t(1 \pm \frac{n}{p}) \mp \frac{(4j-1)n\pi}{4p}] \Big\}. \end{aligned} \quad (13)$$

If $K_{j1} = K_{j2} = K_j$, that is j_1 and j_2 magnetic bodies are in the same degree of demagnetization fault, then formula (13) can be expressed as follows

$$e_{s,A1}(t) = E_S(1 - \frac{K_j}{2p})\sin(2\pi f_e t) - E_S K_j \sum_{n=1}^{\infty} \frac{1}{n\pi} \sin\frac{n\pi}{2p} \sin[2\pi f_e t(1 \pm \frac{n}{p}) \mp \frac{n\pi(2j-1)}{2p}]. \quad (14)$$

So the mathematical model of the slot winding back-EMF is obtained under any single pole demagnetization at any position.

B. Slot winding back-EMF mathematical model under any multiple poles demagnetization.

In the above two sections, the no-load back-EMF mathematical model under any single pole demagnetization have been obtained. Because the no-load back-EMF of the A1 slot and a1 slot windings satisfy the linear superposition principle, so the no-load back-EMF mathematical model of the A1 slot and a1 slot windings under any multiple poles demagnetization fault conditions can be expressed as follows

$$e_{sI,A1}(t) = E_S(1 - \sum_{j=1}^{2p} \frac{K_j}{2p})\sin(2\pi f_e t) - E_S \sum_{n=1}^{\infty} \frac{1}{n\pi} \sin\frac{n\pi}{2p} \cdot \sum_{j=1}^{2p} K_j \sin[2\pi f_e t(1 \pm \frac{n}{p}) \mp \frac{n\pi 2j-1}{2p}], \quad (15)$$

$$\begin{aligned} e_{sI,a1}(t) = E_S(1 - \sum_{j=1}^{2p} \frac{K_j}{2p})\sin(2\pi f_e t - \alpha) - E_S \sum_{n=1}^{\infty} \frac{1}{n\pi} \sin\frac{n\pi}{2p} \times \\ \times \sum_{j=1}^{2p} K_j \sin[2\pi f_e t(1 \pm \frac{n}{p}) \mp \frac{2n\pi j - n(\pi - 2\alpha)}{2p} - \alpha], \end{aligned} \quad (16)$$

where $I = (I_1, \cdots, I_j, \cdots, I_{2p})$; $0 \le K_j \le 1$; if $I_j = 1$, then $K_j = 0$ and $I_j = 0$.

Single phase back-EMF mathematical model under any multiple poles demagnetization.

In order to analyze the mathematical model of the single phase back-EMF, the slot windings of A phase is divided into two groups, and the current direction of A phase is marked with "+" and "-", 16 slots are recorded as a group, such as A11+ and A11-,... , A24+, A24-, 16 slots are recorded as the other group, such as a11+、a11-、…、a24+、a24- , and the electrical angle between the inflow current slot and the

corresponding outflow current slot is π in each group. The A1 slot back-EMF and a1 slot back-EMF can be expressed as (17) and (18) respectively

$$e_{sI,Am}(t)=(-1)^{m-1}E_S(1-\sum_{j=1}^{2p}\frac{K_j}{2p})\sin[2\pi f_e t-\pi(m-1)]-(-1)^{m-1}E_S\sum_{n=1}^{\infty}\frac{1}{n\pi}\sin\frac{n\pi}{2p}\times$$
$$\times\sum_{j=1}^{2p}K_j[\sin 2\pi f_e t(1\pm\frac{n}{p})\mp\frac{(2j-1)n\pi}{2p}-\pi(m-1)(1\pm\frac{n}{p})], \quad (17)$$

$$e_{sI,a1}(t)=(-1)^{m-1}E_S(1-\sum_{j=1}^{2p}\frac{K_j}{2p})\sin(2\pi f_e t-\pi(m-1)-\alpha)-(-1)^{m-1}E_S\sum_{n=1}^{\infty}\frac{1}{n\pi}\sin\frac{n\pi}{2p}\times$$
$$\times\sum_{j=1}^{2p}K_j[\sin 2\pi f_e t(1\pm\frac{n}{p})\mp\frac{2n\pi j-n(\pi-2\alpha)}{2p}-\alpha-\pi(m-1)(1\pm\frac{n}{p})], \quad (18)$$

where $m=1,\ 2,\dots 2p$.

The calculation methods of the single slot winding back-EMF with demagnetization are same, but the single phase back-EMF is related with the connection method of the slot winding. Fig. 2 shows that the two adjacent slot windings belong to one pole and they are connected in series, and the slot windings of different poles are connected in parallel. Therefore, A phase winding back-EMF under any multiple poles demagnetization condition equals to the sum of the two adjacent slot windings back-EMF of any same pole can be expressed

$$e_{AI}(t)=\sum_{m=1}^{2}e_{sI,Am}+e_{sI,am}. \quad (19)$$

The formulas (17) and (18) are substituted into the (19), and the summation order is changed, so the (19) can be expressed as follows

$$e_{AI}(t)=E_S(1-\sum_{j=1}^{2p}\frac{K_j}{2p})(-1)^{m-1}\sum_{m=1}^{2}\{\sin[2\pi f_e t-\pi(m-1)]+\sin[2\pi f_e t-\pi(m-1)-\alpha]\}-$$
$$-E_S(-1)^{m-1}\sum_{n=1}^{\infty}\frac{1}{n\pi}\sin\frac{n\pi}{2p}\sum_{j=1}^{2p}K_j\sum_{m=1}^{2}\Big\{\sin[2\pi f_e t(1\pm\frac{n}{p})\mp\frac{(2j-1)n\pi}{2p}- \quad (20)$$
$$-\pi(m-1)(1\pm\frac{n}{p})]+\sin[2\pi f_e t(1\pm\frac{n}{p})\mp\frac{2n\pi j-n(\pi-2\alpha)}{2p}-\alpha-\pi(m-1)(1\pm\frac{n}{p})]\Big\}.$$

The sum of the first item in the formula (20) is proved as:

$$e_{AI}(t)=2E_S(1-\sum_{j=1}^{2p}\frac{K_j}{2p})[\sin 2\pi f_e t+\sin(2\pi f_e t-\alpha). \quad (21)$$

The comparison no-load back-EMF mathematical model of A1 slot, a1 slot and A phase windings shows that the electric potential of the slot winding is changed when demagnetization fault occurred, and the fault specific location can be reflected, that is the amplitude peaks or troughs correspond to the demagnetization pole, and the serious demagnetization of pole can be reflected by the extent of its amplitude decreases; The fundamental component of single phase back-EMF amplitude decreases with any single pole or any multiple poles demagnetization fault and reflects of whole demagnetization severity.

Comparison mathematical model computation with simulation model computation results.

In order to verify the back-EMF mathematical model of the PMSM demagnetization fault, the mathematical model of the A1 slot winding back-EMF under pole 1 and 2 respectively at 25% and 50% demagnetization is compared with the FEM simulation results, as it is shown in Fig. 5, *a*. When at the PMSM poles 1 and 2 of electric vehicles respectively occurred 25% and 50%, demagnetization, the simulation results of A-phase back-EMF of and mathematical model of calculation results are shown in Fig. 5, *b*.

It can be seen from Fig. 5, *b* the A phase has no obvious change in the electric potential and the peak value is decreased. The waveform of single phase back-EMF can not reflect the specific position of the demagnetization pole and can reflect only the total demagnetization effect. The results of the single phase back-EMF mathematical model are basically consistent with the results of FEM simulation, which verifies the validity of the mathematical model.

Conclusions.

The demagnetization fault for EV PMSM is studied in the paper, the mathematical model of the single slot and the single phase no-load back-EMF is developed for any single magnet and pole, as well as any two adjacent magnets and any multiple poles with different degree of demagnetization. The model has nothing to do with the rotor magnet structure. The FEM simulation is carried out to verify the mathematical model. When the pole demagnetization fault occurs, the following conclusions can be made:

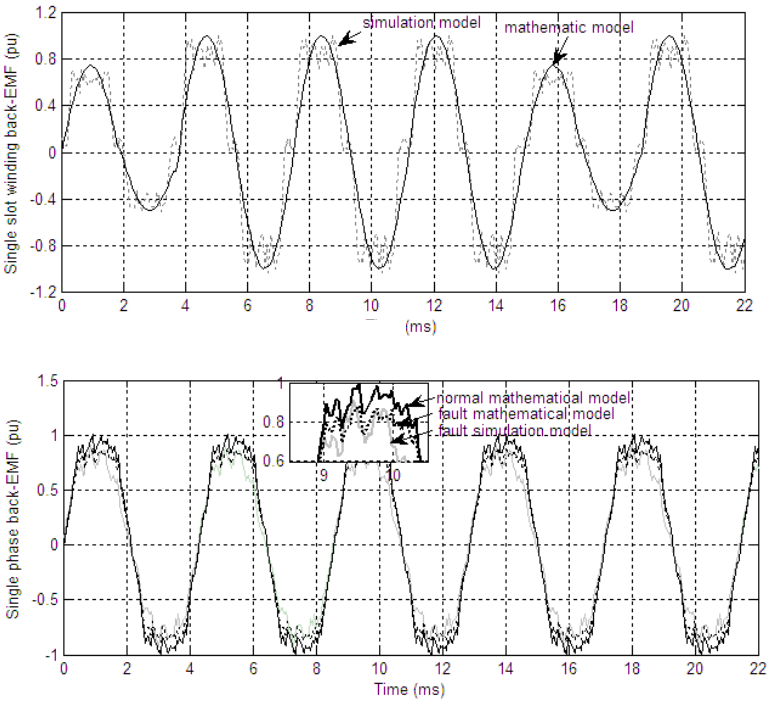

− the single slot winding back EMF waveform changes, the decrease wave peak or trough can reflect demagnetization pole location, and the value of amplitude decrease can reflect the severity of demagnetization fault.

− the single phase back-EMF waveform can't reflect the specific position of the demagnetization pole, and its fundamental component amplitude is also reduced, but can reflect only the demagnetization severity of all permanent magnets.

1. *Antonio Garcia Espinosa, Javier A. Rosero, Jordi Cu-sido, et al.* Fault detection by means of Hilbert-huang transform of the stator current in a PMSM with demagnetization // IEEE Transactions on Energy Conversion. – 2010. – No 2. – Pp. 312–318.

2. *Jongman Hong, Doosoo Hyun, Sang Bin Lee, et al.* Automated monitoring of magnet quality for permanent magnet synchronous motors at Standstill // IEEE Transaction on Industry Applications. – 2010. – No 4. – Pp. 1397–1405.

3. *Jordi-Roger Riba Ruiz, Javier A.Rosero, Antonio Gar-cia Espinosa, et al.* Detection of demagnetization faults in permanent-magnet synchronous motors under nonstationary conditions // IEEE Transactions on Magnetics. – 2009. – No 7. – Pp. 2961–2969.

4. *Julio-Cesar Urresty, Jordi-Roger Riba, Miguel Delgad-o, et al.* Detection of demagnetization faults in surface mounted permanent magnet synchronous motors by means of the zero-sequence Voltage Component // IEEE Transactions on Energy Conversion. – 2012. – No 1. – Pp. 42–51.

5. *Leila Parsa, Hamid A., Toliyat.* Fault-tolerant interior permanent magnet machines for hybrid electric vehicle applications // IEEE Transaction on Vehicular Technology. – 2007. – No 4. – Pp. 1546–1552.

6. *LU Weifu, LIU Mingji, LUO Yingli, et al.* Demagnetization field analysis and calculation for line-start permanent magnet synchronous motor during start process // Proceedings of the CSEE. – 2011. – No 15. – Pp. 53–60.

7. *Marius Rosu, Július Saitz, Antero Arkkio.* Hysteresis model for finite-element analysis of permanent demagnetization in a large synchronous motor under a fault condition // IEEE Transactions on Magnetics. – 2005. – No 6. – Pp. 2118–2123.

8. *Miguel Delgado Prieto, Antonio Garcia Espinosa, Jordi Roger Riba Ruiz, et al.* Feature extraction of demagnetization faults in permanent-magnet synchronous motors based on box-counting fractal dimension // IEEE Transactions on Industry Electronics. – 2011. – No 5. – Pp. 923–932.

9. *Sami Ruoho, Emad Dlala, Antero Arkkio.* Comparison of demagnetization models for finite-element analysis of permanent-magnet synchronous machine // IEEE Transactions on Magnetics. – 2007. – No 11. – Pp. 3964–3968.

УДК 621.3

АНАЛИЗ ЭФФЕКТА РАЗМАГНИЧИВАНИЯ ПРОТИВОДЕЙСТВУЮЩЕЙ ЭЛЕКТРОДВИЖУЩЕЙ СИЛЫ СИНХРОННОГО ДВИГАТЕЛЯ С ПОСТОЯННЫМИ МАГНИТАМИ С ПОМОЩЬЮ МАТЕМАТИЧЕСКОЙ МОДЕЛИ, ОСНОВАННОЙ НА ПРИНЦИПЕ СУПЕРПОЗИЦИИ ПОЛЕЙ

Zhiyan Zhang[1], Zehui Xie[1], Hongzhong Ma[2], Qin Zhong[3]
[1] – Zhengzhou University of Light Industry, College of Electrical and Information Engineering, Dongfeng Road No. 5 Zhengzhou City Henan Province China.
e-mail: 2004074@zzuli.edu.cn; 2000002@zzuli.edu.cn
[2] – College of Energy and Electrical Engineering, Hohai University, Fucheng West Road No. 8 Nanjing City Jiangsu Province, 210098, China. e-mail: Hongzhong Ma@163.com
[3] – Huzhou Power Company, Electric Power Company of Zhejiang Province, Fenghuang Road No.777 Huzhou City Zhejiang Province, 313000, China. e-mail: hhupszq@163.com

В соответствии с принципом суперпозиции магнитного поля и характеристиками серий прямоугольных сигналов противодействующая электродвижущая сила синхронного двигателя с постоянными магнитами (СДПМ) в состоянии эффекта размагничивания раскладывается на рабочий компонент и компонент эффекта размагничивания. В статье представлена математическая модель однопазовой и однофазной противодействующей электродвижущей силы без нагрузки, когда при любом магнитном теле, любом полюсе или нескольких полюсах возникает эффект размагничивания. В статье сопоставлены результаты математической модели противодействующей электродвижущей силы СДПМ мощностью 42 кВт, который имеет 8 полюсов и V-образную форму постоянных магнитов, с результатами имитационного моделирования методом конечных элементов, что позволило подтвердить математическую модель. Результаты показывают, что форма сигнала противодействующей электродвижущей силы пазовой части обмотки может отражать определённое положение полюсов размагничивания. Форма сигнала однофазной противодействующей электродвижущей силы может отражать только условия размагничивания всех полюсов, но не может определять конкретное положение полюсов размагничивания. Библ. 9, рис. 5.

Ключевые слова: СДПМ (синхронный двигатель с постоянным магнитом); сбой размагничивания; противодействующая электродвижущая сила; математическая модель; модели для имитационного моделирования.

УДК 621.3

АНАЛІЗ ЕФЕКТУ РОЗМАГНІЧУВАННЯ ПРОТИДІЮЧОЇ ЕЛЕКТРОРУШІЙНОЇ СИЛИ СИНХРОННОГО ДВИГУНА З ПОСТІЙНИМИ МАГНІТАМИ ЗА ДОПОМОГОЮ МАТЕМАТИЧНОЇ МОДЕЛІ, ЗАСНОВАНОЇ НА НА ПРИНЦИПІ СУПЕРПОЗИЦІЇ ПОЛІВ

Zhiyan Zhang[1], Zehui Xie[1], Hongzhong Ma[2], Qin Zhong[3]
[1] – Zhengzhou University of Light Industry, College of Electrical and Information Engineering, Dongfeng Road No. 5 Zhengzhou City Henan Province China.
e-mail: 2004074@zzuli.edu.cn ; 2000002@zzuli.edu.cn
[2] – College of Energy and Electrical Engineering, Hohai University, Fucheng West Road No. 8 Nanjing City Jiangsu Province, 210098, China. e-mail: Hongzhong Ma@163.com
[3] – Huzhou Power Company, Electric Power Company of Zhejiang Province, Fenghuang Road No.777 Huzhou City Zhejiang Province, 313000, China. e-mail: hhupszq@163.com

Відповідно до принципу суперпозиції магнітного поля і характеристик серій прямокутних сигналів протидіюча електрорушійна сила синхронного двигуна з постійними магнітами (СДПМ) у стані ефекту розмагнічування розкладається на робочий компонент і компонент ефекту розмагнічування. У статті представлено математичну модель однопазової та однофазної протидіючої електрорушійної сили без навантаження, коли при будь-якому магнітному тілі, будь-якому одному або при декількох полюсах виникає ефект розмагнічування. У статті співставлено результати математичної моделі протидіючої електрорушійної сили СДПМ потужністю 42 кВт, який має 8 полюсів та V-подібну форму постійних магнітів, з результатами моделі для імітаційного моделювання методом кінцевих елементів, що дозволило перевірити і підтвердити математичну модель. Результати показують, що форма сигналу протидіючої електрорушійної сили пазової частини обмотки може відображати певне положення полюсів розмагнічування. Форма сигналу однофазної протидіючої електрорушійної сили може відображати тільки умови розмагнічування всіх полюсів, проте не може визначати конкретне положення полюсів розмагнічування. Бібл. 9, рис. 5.

Ключові слова: СДПМ (синхронний двигун з постійним магнітом); збій розмагнічування; протидіюча електрорушійна сила; математична модель; модель для імітаційного моделювання.

Надійшла 18.11.2015
Остаточний варіант 04.01.2016